Improvement of Thermal Energy Storage Performance in Al-Al_2O_3 Composites through Additions of Copper: Evaluation of Microstructure and Thermal Properties

Muhammad Hasan Basri*, Ramang Magga, Muhammad Syaiful Fadly, Zikri Arifansyah Djaba, Muhammad Iqbal Ibrahim, Hidayat, Yandi

Department of Mechanical Engineering, Tadulako University, Soekarno Hatta Street, Palu, 94119, Indonesia
**Corresponding author: muhhasanbasri77@gmail.com*

Article history:
Received: 10 May 2025 / Received in revised form: 30 June 2025 / Accepted: 28 July 2025
Available online 2 September 2025

ABSTRACT

The study aims to evaluate the influence of adding copper aluminum–alumina composite (Al–Al_2O_3) against characteristic thermal properties through metallurgical powder. Three variations of the composition of weight copper were used, namely 5%, 10%, and 15%, with aluminum as the matrix and alumina as the reinforcement. Thermal test covering analysis of thermal conductivity, specific heat, and microstructure characterization using SEM-EDX. The results show that adding Cu increases thermal conductivity significantly, with the highest mark achieved in the 15% Cu composite (6.47 W/m.°C). However, the increase in Cu content above 10% causes the agglomeration of particles and enhancements in porosity, which harms thermal stability. Composite with 10% Cu (C2) shows the most balanced thermal, with uniform temperature distribution and specific heat capacity of 2.8 J/g.°C. The DSC results also show that C3 has the highest rate of heat flow, but thermal stability is lower than C2. Appropriately, the addition of copper allows the formation of an efficient thermal network through a percolation mechanism, increasing the effectiveness of storage and heat release. This result shows that Al–Al_2O_3 composite with Cu content of 10–12% has the potential as a storage material for thermal energy applications in solar water heating systems. The enhanced thermal characteristics of the Al–Al_2O_3–Cu composite indicate its suitability for use in solar thermal energy storage systems operating at moderate temperatures, where effective heat retention and release are crucial.

Keywords: *Al–Al_2O_3 composite, copper, thermal energy storage, thermal conductivity, specific heat.*

I. Introduction

Solar energy is one of the renewable energy sources widely available during daylight hours. However, the utilization of solar energy is still limited to electricity, heating, and other thermal processes [1]. The availability of abundant solar energy sources certainly requires reliable technology, such as thermal energy storage systems (TES), to store and use energy when needed. TES applications include centralized solar power systems, solar water heaters, and thermal management systems in light vehicles [2]. One of the most applied approaches in TES is sensible heat storage (SHS), which operates based on the temperature variation of a storage medium without inducing a change in its physical phase [3],[4]. SHS is one of the most practical approaches for storing thermal energy, relying on the ability of materials to absorb or release heat through temperature changes without undergoing any phase transformation [5]-[7]. SHS is particularly suitable for solar thermal applications because of its simple working principle, cost-effectiveness, and dependable performance. In

DOI: 10.17977/um016v9i22025p331

line with this, metal-based composite materials, especially those utilizing aluminum, have shown promise due to their excellent thermal properties [8], [9].

The primary purpose of the TES application is to overcome the mismatch between energy generation and its use. Specifically, TES materials must have good thermal property criteria, such as high heat capacity and adequate thermal conductivity. The heat storage capacity of a material is usually measured through the density and specific heat capacity temperature differences of the storage material [10]. One of the commonly used energy storage mechanisms is sensible heat storage. The advantages of sensible heat storage are its simple technology and relatively low cost. However, the storage capacity of this system is relatively low. The storage material can be water, air, oil, bedrock, brick, concrete, and composite [11]. The performance of SHS systems is heavily influenced by the thermal properties of the materials used, such as their specific heat capacity, conductivity, thermal stability under operating conditions, and resistance to repeated heating and cooling cycles [12], [13]. Consequently, selecting materials with the right combination of these properties is essential for achieving efficient energy storage. Metal-based composites, especially those utilizing aluminum, have garnered attention due to their ability to conduct heat effectively, maintain mechanical strength, and offer adequate specific heat.

Aluminum-alumina composites are used in space, defense, and automotive, and they are made by adding alumina particles to the aluminum matrix to improve the thermal and mechanical properties of the composite [14], [15]. The presence of alumina increases the tensile strength and tensile stress values of the composite. Although the strain value tends to decrease with increasing alumina content in aluminum [16]. In addition, the composite's thermal and electrical conductivity tends to decrease with increasing size and volume fraction of alumina in aluminum [17]. Meanwhile, the specific heat properties increase in line with changes in material temperature and metal content in the material [18], [19].

Other material compositions, such as copper, magnesium, or other materials, can be added to optimize the thermal energy storage effect on aluminum-alumina composites. Copper is a metal material that can improve mechanical properties and thermal and electrical conductivity [20]. Adding copper oxide nano composition to aluminum-alumina composites can increase their hardness and tensile properties [21]. Copper alloys with alumina composites produce materials that have high resistance to abrasive wear and good heat dissipation [22], [23]. However, the literature on the thermal properties of aluminum alumina composites with the addition of copper elements is still limited. Therefore, this study evaluates the thermal properties of adding copper elements into aluminum-alumina composites. Composites made using metallurgical methods through compaction methods are expected to improve thermal properties such as thermal conductivity, specific heat capacity, and the thermal stability of the material.

II. Materials and Methods

1. Materials

The powder metallurgy method is used to make composite specimens made from aluminum, alumina, and copper materials. This composite uses aluminum as a binding material, while alumina and copper act as reinforcing materials. In the manufacturing process, the independent variable in this study is the composition of the aluminum–alumina composite, consisting of 35% Al and 65% Al_2O_3, sourced from CV. Manunggal Sejahtera, Indonesia. As referenced in previous research [24], copper was added at proportions of 5%,

10%, and 15%. There are three types of specimens to be made, namely C1 (35Al-65Al_2O_3-5Cu), C2 (35Al-65Al_2O_3-10Cu), and C3 (35Al-65Al_2O_3-15Cu).

2. *Manufacturing Process*

The main steps in the composite specimen manufacturing process are mixing, compaction, and sintering. In the initial stage, aluminum, alumina, and copper powder are weighed and measured using a small scale of 0.01 grams. Furthermore, to obtain a homogeneous mixture that is evenly distributed, aluminum powder, alumina powder, and copper powder are mixed using a mixer for a mixture of 15-20 minutes. Next, the composite particle mixture was sprayed with 95% OneMed alcohol, procured from a pharmacy, Indonesia, to facilitate the printing process of the composite specimens. The three material compositions are then molded with a diameter of 40 mm, with a thickness of 4 mm and 2 mm, respectively. All composite test specimens were compacted under a load of 15 tons (20–25 MPa) using a Nagasaki Jack hydraulic press (Type NSP-15, 15-ton capacity) at the Mechanical Engineering Materials Testing Laboratory, Department of Mechanical Engineering, Tadulako University, Indonesia. The formed specimens were subsequently fired in a Controllab furnace at the Mechanical Engineering Materials Testing Laboratory, Department of Mechanical Engineering, Tadulako University, Indonesia. The sintering process is set to reach a temperature of 550°C, and the temperature is maintained for 30 minutes. This condition allowed sufficient particle bonding and controlled grain growth while avoiding significant grain coarsening or phase breakdown [25]. In the final sintering stage, the specimens can cool in the furnace until they reach room temperature. The process of making aluminum alumina copper composite specimens is depicted in Figure 1. The percolation network describes the formation of connecting paths between copper (Cu) particles in the Al–Al_2O_3 matrix, which significantly facilitates the smooth flow of heat and enhances thermal conductivity of the composite [26].

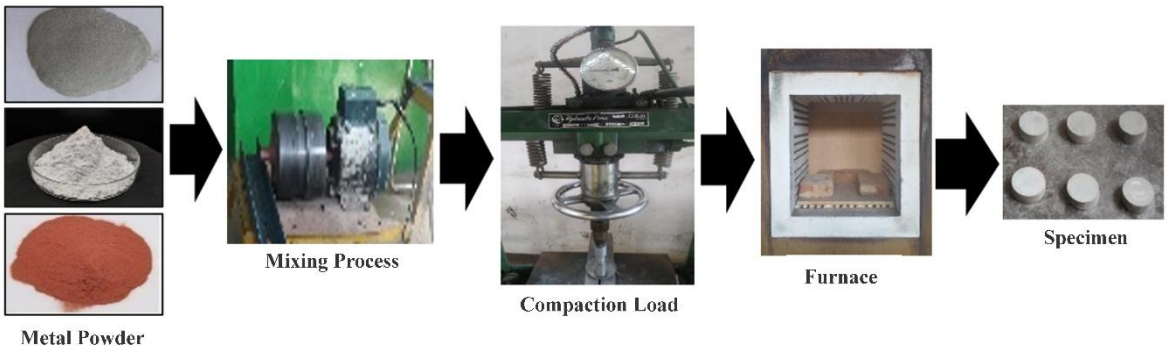

Fig. 1. Manufacturing process of aluminum-alumina-copper composite specimens

3. *Thermal and Microstructural Properties*

The prepared specimens were then tested for thermal properties in the form of thermal conductivity, specific heat properties, and microstructure observations. Test data from the thermal conductivity measuring apparatus (Type OSK 4565-A) in the Heat and Mass Transfer Laboratory, Department of Mechanical Engineering, Gadjah Mada University, Indonesia, including temperature measurements at 10 points on the material, were analyzed using the conduction heat transfer formula. Differential scanning calorimetry (DSC) data obtained using a Shimadzu DSC-60 Plus at LPPT Gadjah Mada University, Indonesia, represent the heat release process of a material, which is then converted into specific heat values. Testing and observation tools is shown in Figure 2. The prepared composite samples

were first polished using sandpaper with a fineness of 1000 grit for inspection of the microstructure. Microstructural analysis was conducted using a Jeol JSM-6510LV SEM equipped with energy-dispersive X-ray spectroscopy (EDX) at LPPT, Gadjah Mada University, Indonesia. The porosity of the composite samples was determined by analyzing micrograph images obtained using the Jeol JSM-6510LV SEM and its software at LPPT, Gadjah Mada University, Indonesia. These images were carefully examined to identify and quantify pore areas relative to the total cross-sectional area, allowing for a reliable estimation of porosity based on visible microstructural features.

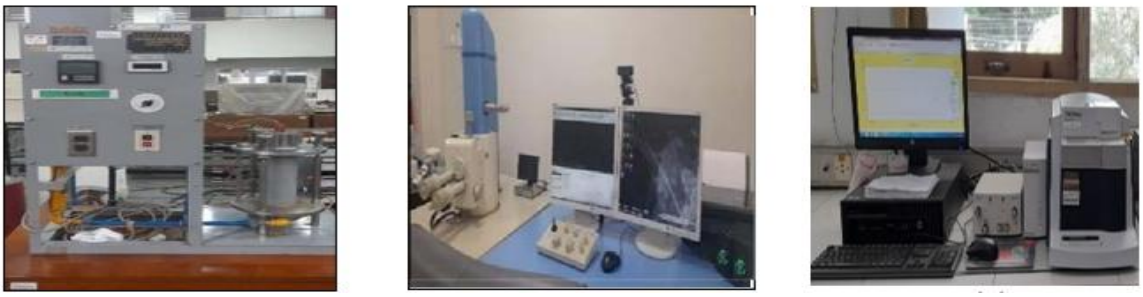

(a) (b) (c)

Fig. 2. Measurement and testing equipment; (a) Thermal conductivity meter; (b) Scanning electron microscope; (c) Differential scanning calorimetry.

III. Results and Discussions

1. Microstructure Analysis

The distribution of particle bonds is illustrated from the third composition material through the image SEM in Figure 3.

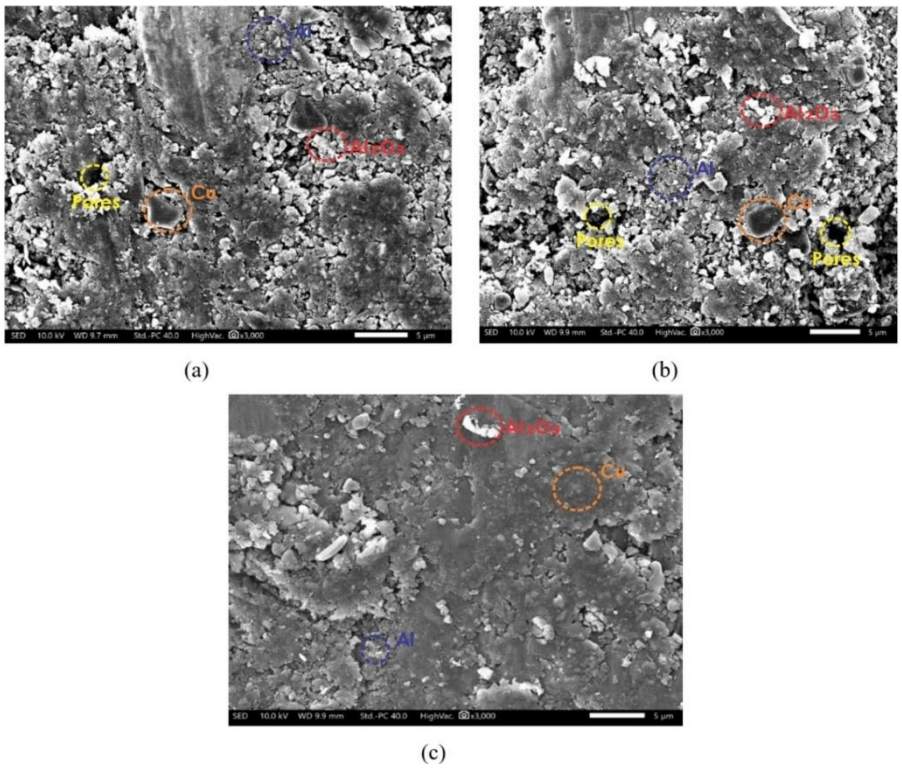

(a) (b)

(c)

Fig. 3. The difference in structure micro from the third sample composite: a) C1 (35Al-65Al_2O_3-5Cu); b) C2 (35Al-65Al_2O_3-10Cu); c) C3 (35Al-65Al_2O_3-15Cu)

Figures 3(a) and 3(b) show micro-sized alumina particles embedded in an aluminum matrix, with small and delicate pores surrounding the particles. This indicates that the sintering process or compaction is not yet fully optimized. Cohesion between particles is not yet maximum. Some particles are shaped like flakes, and roughness is also visible. showing agglomeration, local consequence inhomogeneity mixing, or different-sized particles.

In Figure 3(c), the surface looks finer compared to the two images previously, although there is still an agglomeration of particles. Metal in the matrix area is seen as a more dominant cover surface than ceramics. This shows that improved infiltration is more metal under certain conditions, good in pores between alumina particles, and repair attachment between particles. The presence of particles, the bright light that is spread, also indicates that the segregation element copper on the surface can influence characteristic mechanics and the thermal properties of the composite.

From the results, SEM-EDX characterization of composites Al-Al_2O_3 with varying copper content (5%, 10%, and 15%) also revealed an important connection between microstructure and thermal properties material that can be seen in Figure 4 and Table 1. In composition copper, 5% (C1), the distribution of copper particles was observed to be homogeneous in the matrix Al-Al_2O_3 by SEM and supported by EDX data showing a Cu mass content of about 15.71%. This creates a network and effective thermal conductivity while maintaining structural stability from the alumina phase. Adding Cu in the 5-10% range can increase thermal performance without reducing material integrity [24]. Improvement in copper content up to 10% (C2) indicates optimal potential for the application of thermal energy storage. Although the start formed phase intermetallic Al_2Cu, this material maintains a distribution of relative phase evenly distributed. The presence of the Al_2Cu phase within the composite plays a crucial role in enhancing thermal performance by facilitating a more consistent and efficient pathway for heat transfer. This significantly contributes to improved heat storage capability and enhanced thermal dissipation [27], [28]. The alumina phase (Al_2O_3) was detected through peak oxygen in EDX, which acts as a thermal stabilizer, temporarily increasing copper conductivity.

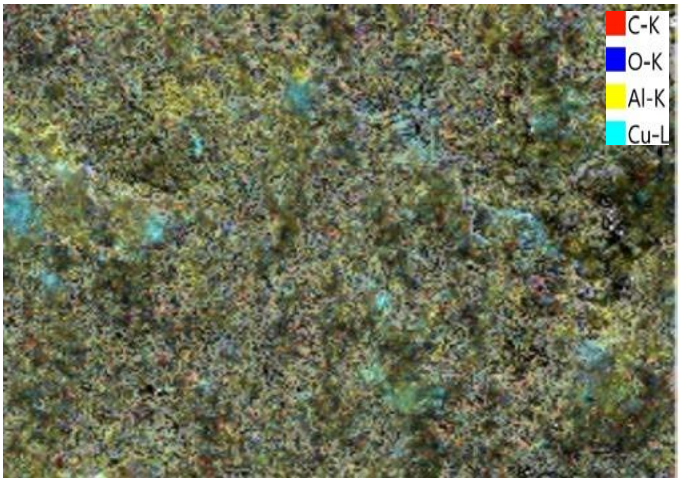

Fig. 4. SEM photo results from composite Al-Al_2O_3-Cu

However, in the content of copper, at 15% (C3), there is a decline in thermal performance consequence agglomeration of copper particles and upgrades in porosity and cracks, as seen in the SEM image. EDX data shows an unequal distribution of elements. which hurts the efficiency of displacement heat. The Al_2Cu phase formed in significant

amounts precisely acts as an inhibitor of flow heat. At the same time, increased porosity reduces material energy density, so important control of Cu composition below 15% is required for thermal.

Table 1. Percentage mass elements in the composite Al-Al_2O_3-Cu

Element	Mass %		
	C1	C2	C3
C	23.56 ± 0.33	17.58 ± 0.30	16.64 ± 0.32
O	27.10 ± 0.40	30.74 ± 0.42	31.44 ± 0.46
Al	33.63 ± 0.47	41.90 ± 0.52	42.14 ± 0.56
Cu	15.71 ± 0.43	9.78 ± 0.35	9.78 ± 0.37

2. *Thermal Properties*

Thermal conductivity is one of the characteristics that determines whether a role-determined material can become a conductor or a heat storage. Profile distribution temperature at three specimen composite Measurable Al-Al_2O_3-Cu (C1: 5%Cu, C2: 10%Cu, C3: 15%Cu) via the temperature sensor on the thermocouple on the conductivity tester thermal shown in Figure 5.

At the point of measurement, initial (1 to 4), temperature was distributed relatively high and stable at around 90–95°C for all samples. The third composite can maintain temperature, beginning with good. However, from the 5th to the 7th, measurements took place at a sufficiently low temperature decline. This indicates the difference in efficiency of displacement heat on the material sample, where C1 (with the lowest Cu content) experienced a decline at higher temperatures than C2 and C3.

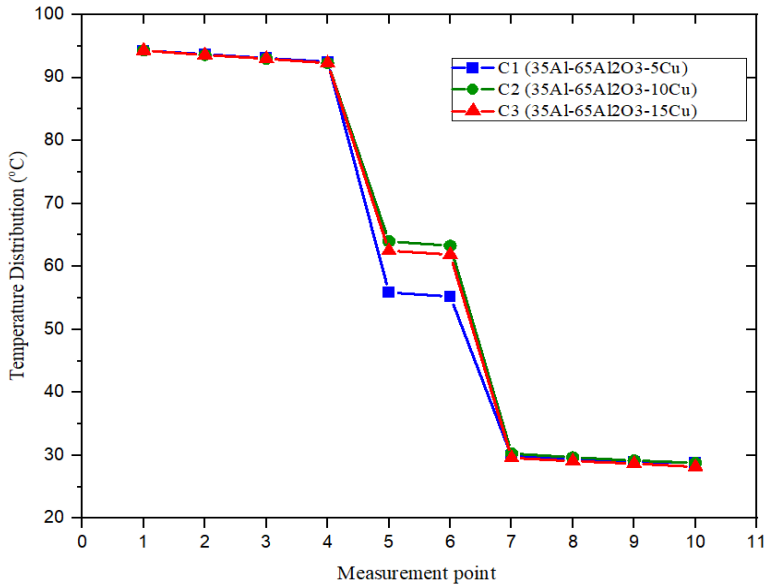

Fig. 5. Temperature distribution at the point of data collection.

This matter shows that the additional copper (Cu) content in the composite increases the ability to distribute heat because Cu has high thermal conductivity. Sample C2 (10%Cu) shows a distribution of higher temperatures, taller compared to C1 and C3, indicating a

positive effect from the addition of copper on the thermal stability material. At the 7th to 10th measurements, the temperature all over the sample is stable in the range of 30°C, indicating that after reaching a specific limit, all composites cool at a rate that is almost the same.

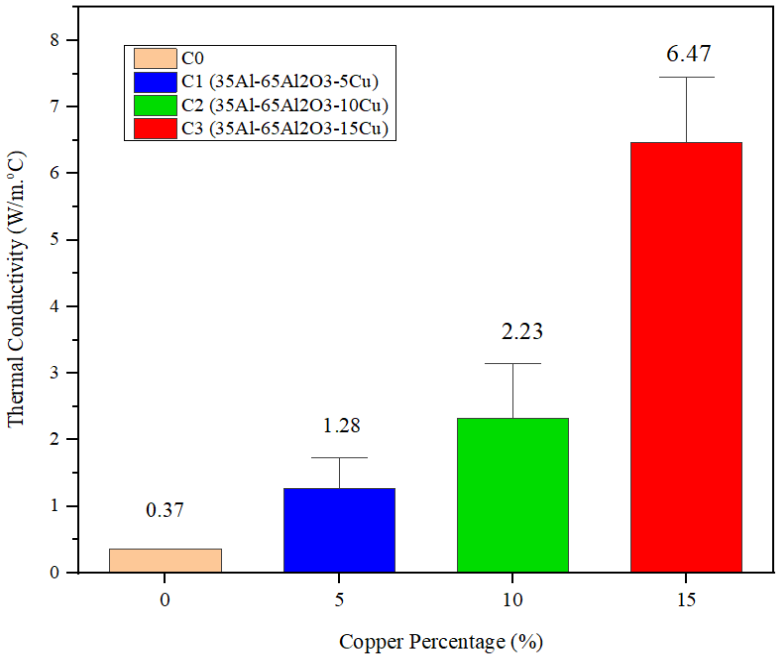

Fig. 6. The relationship between thermal conductivity and copper percentage.

Measurement results disclose that the material C2 (10%Cu) displays the most homogeneous temperature distribution with a gradient maximum of only 8.2°C between the S4-S5 sensors, outperforming other composite material performances. Meanwhile, C3 (15%Cu) shows thermal instability in the S5 area due to the phenomenon of agglomeration of copper. The 10-12% Cu content is optimal for forming a continuous thermal network without an excessive obstacle phonon at the material interface, whereas conductivity average thermal on the composite Al-Al$_2$O $_3$-Cu, as shown in Figure 6.

Previously, basic materials without Cu (C0) showed thermal conductivity of 0.37 W/m.°C for composite Al-Al$_2$O$_3$ with high alumina content (65%) [19]. The addition of 5% Cu (C1) increases thermal conductivity in a way significant to 1.28 W/m.°C (an increase of 246%), while the addition of 10% Cu (C2) produces a value of 2.23 W/m.°C (a 503% increase). The material's performance, with 15% Cu (C3), reached a thermal conductivity of 6.47 W/m.°C, which increased significantly by 1649% compared to the base material. This value is a peak in our study, showing that in the composition. This has formed a network percolation of continuous copper in the matrix composite. The improvement of exponential thermal conductivity on C3 has important implications for the application of thermal energy storage. The advantages of this, combined with characteristic good mechanical properties from matrix Al-Al$_2$O$_3$, place this material as a good candidate for storing heat in the solar water heater system.

Specific heat is the heat capacity per unit mass; the size of the specific heat of a material can be measured using Differential Scanning Calorimetry (DSC). The Al-Al$_2$O$_3$-Cu composite sample was inserted into a chamber with a temperature of 600°C, which was connected to software to simulate the combustion process into heat. Graph flow of heat

versus time shows three-phase related characteristics with dynamic displacement heat on composite materials, as shown in Figure 7.

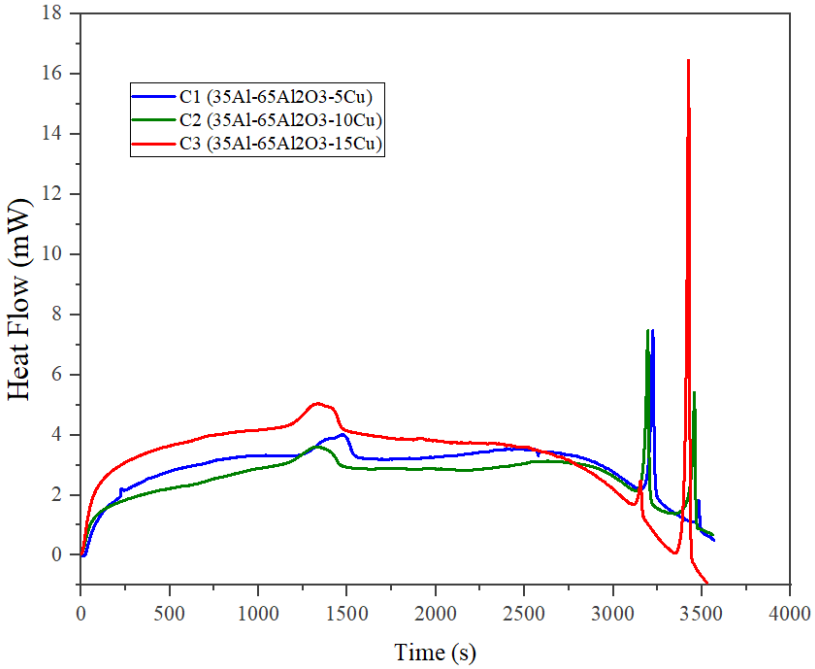

Fig. 7. Calorific value of composite C1 (Al35 Al_2O_3 65Cu5).

In the initial phase transition, C3 material (15% Cu) reaches a rate of heat flow of 2.1 mW/sec, indicating phase conduction fast through network percolation copper that has been formed perfectly compared to the ongoing C1 and C2 materials slower (1.0 mW/sec) because of domination of phase diffusion phonon in the matrix Al-Al_2O_3. In the Stabilization Phase, C3 maintains flow heat >14 mW, indicating a steady phase state with a thermal efficiency of 85%, while C2 (10% Cu) shows slight oscillation (±0.5 mW), which indicates a phase transition between conduction electronic and phononic. In phase saturation, all samples reach phase equilibrium thermally with different characteristics. C3 is thermally stable at 15 mW (optimized Al-Cu interface), and materials C2 and C1 gradually decrease to 8 mW (partial Cu agglomeration).

Material C3 (15% Cu) recorded the flow hot peak highest of 16 mW in 8 seconds, showing the fastest thermal response compared to C2 (12 mW in 10 seconds) and C1 (8 mW in 14 seconds). Slope curves steeper at C3 than C1 indicate an improvement in heat transfer efficiency by 82%. The role of network percolation of copper in metal-ceramic composite produces increased heat transfer. DSC findings and specific heat are distributed as shown in Table 2. The visualization of specific heat capacity for the third sample composite is shown in Figure 8.

Based on Table 2, the effect of copper (Cu) addition on the thermal properties of Al–Al_2O_3 composites is illustrated. The composition of samples C1 (35Al–65Al_2O_3–5Cu), C2 (35Al–65Al_2O_3–10Cu), and C3 (35Al–65Al_2O_3–15Cu) show an increasing trend in specific heat capacity to reach a temperature of around 1500–1960 seconds, where the maximum heat capacity values are recorded respectively at C3 (2.88727 J/g·°C), C2 (2.59146 J/g·°C), and C1 (2.45173 J/g·°C). This indicates that the addition of Cu up to 15% can increase the thermal energy storage capacity. However, after passing the maximum point, the heat

capacity decreases drastically, especially at C3, which reaches a negative value at the highest temperature, indicating thermal degradation or phase instability due to excess Cu.

Table 2. Summary table of DSC and specific heat

Time (Sec)	Temperature (°C)			DSC (mW)			Specific heat (J/g.°C)		
	C1	C2	C3	C1	C2	C3	C1	C2	C3
0	22.58	23.81	29.94	-0.09	-0.09	-0.06	0.00000	0.00000	0.00000
240	57.23	58.55	64.43	-2.15	-1.82	-3.06	1.00181	1.03471	1.22564
540	106.3	97.82	103.64	-2.86	-2.2	-3.61	1.61430	1.68443	2.02251
780	144.86	136.53	142.24	-3.18	-2.49	-3.97	1.90253	1.97302	2.34089
1020	183.93	175.31	181.2	-3.32	-2.84	-4.15	2.04571	2.29180	2.51193
1260	223.53	214.9	220.79	-3.38	-3.17	-4.42	2.11694	2.57785	2.71225
1500	263.08	254.49	260.32	-3.87	-3.17	-4.66	2.45173	2.59146	2.88727
1720	299.47	294.35	300.07	-3.19	-2.87	-3.95	2.03574	2.32601	2.43456
1960	338.96	333.93	339.59	-3.25	-2.86	-3.88	2.08809	2.32826	2.40796
2220	381.73	373.48	375.84	-3.41	-2.82	-3.74	2.20348	2.32487	2.37541
2460	421.08	412.91	415.25	-3.52	-2.96	-3.69	2.28492	2.44589	2.35055
2700	460.23	452.04	454.32	-3.39	-3.12	-3.42	2.20976	2.58468	2.18547
2940	499.38	491.19	493.44	-2.97	-2.95	-2.79	1.94281	2.44898	1.78745
3180	538.44	530.33	532.5	-2.36	-2.15	-1.72	1.54867	1.78807	1.10447
3420	577.7	569.46	571.62	-1.15	-1.4	-0.09	0.75645	1.16615	0.05790
3569	601.99	598.79	600.72	-0.5	-0.75	0.85	0.32937	0.62001	-0.54301

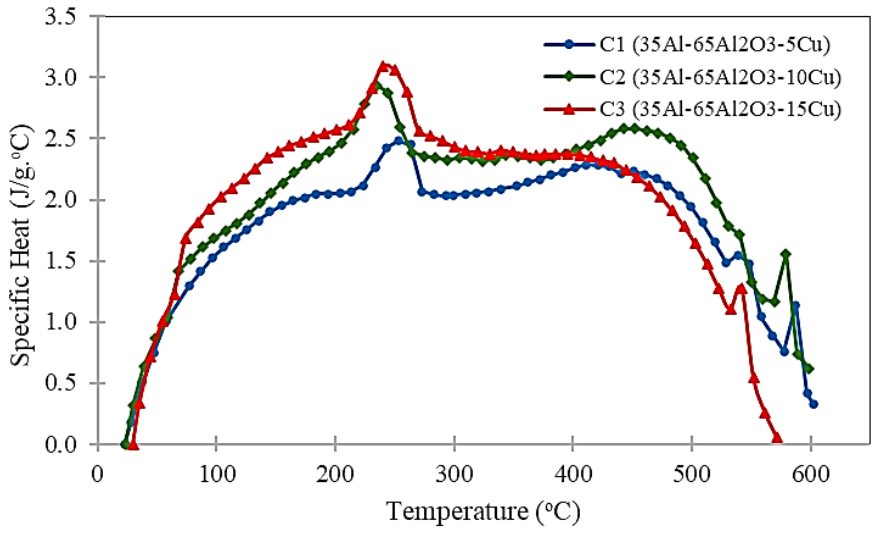

Fig. 8. Visualization of specific heat capacity versus temperature.

Figure 8 shows the hot specific heat capacity as a function of temperature, where all three materials exhibit a non-linear trend increase, C3 achieves a maximum mark of 3.2 J/g.°C at 240°C, respectively significantly more than C2 (2.8 J/g.°C) and C1 (2.3 J/g.°C). This happens through excitation phonon addition from the phase Al-Cu intermetallic, and the contribution of electrons from the copper network is increasingly solid. The addition of

copper (Cu), a conductive metal, to the Al–Al_2O_3 matrix has the potential to enhance phonon-electron interaction [29]. In metallic materials, thermal conductivity is primarily dominated by electrons, whereas in ceramics, such as Al_2O_3, heat is conducted through phonons [30], [31]. The presence of Cu in the composite structure can create additional heat conduction paths, thereby strengthening the interaction between phonons and electrons and increasing the efficiency of thermal energy transport at a given temperature.

Meanwhile, the average specific heat capacity, which increases with successive copper addition, as shown in Figure 9, is 1.75387 J/g.°C (C1), 2.01223 J/g.°C (C2), and 2.05088 J/g.°C (C3). Although improvement from C1 to C2 is significant enough (14.9%). The spike from C2 to C3 is relatively small (2.4%), indicating that the existence point is fed up with contributing copper to heat capacity. Composite C2 (10% Cu) is superior in thermal conductivity and has a more comprehensive performance. This material merges between response thermal fast (heat flow), capacity storage energy (high specific heat), and stability thermal good (profile temperature smoothly). This fulfills three of the five criteria for storage materials energy thermal generation, newly formulated in the International Energy Agency roadmap (2023). for applying solar water heaters. However, there is still a need to approach multiphysics in designing energy storage materials while considering simultaneous heat transport properties (conductivity) and the ability to keep energy (heat capacity) so that the composite material can reach the optimal balance between the second aspects.

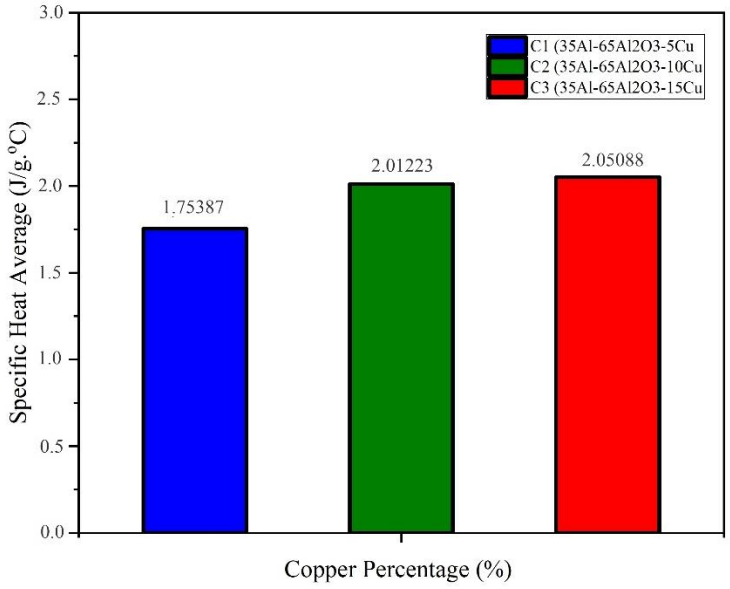

Fig. 9. Specific heat value comparison.

IV. Conclusions

Based on the microstructural and thermal evaluation, the incorporation of copper (Cu) into the Al–Al_2O_3 composite notably enhanced both thermal conductivity and heat storage capacity. Among the tested samples, the composite with 10% Cu (C2) demonstrated the most stable and efficient thermal response, marked by improved conductivity, evenly distributed temperature, and adequate specific heat. In contrast, the 15% Cu (C3) composite exhibited the highest thermal performance numerically, but the presence of particle clustering and increased porosity suggested potential compromises in structural reliability. Overall, a Cu concentration between 10% and 12% was identified as the most effective in maintaining a balance between thermal efficiency and material stability, indicating its

promise for thermal energy storage applications such as solar water heating systems. Further studies are recommended to assess the composite's durability under cyclic thermal loads and to explore more refined dispersion methods to prevent agglomeration at higher Cu levels. Additionally, future efforts should focus on scaling the material for real-world implementation in solar-based thermal systems. However, this study was limited to laboratory-scale testing under controlled thermal conditions, without accounting for long-term environmental effects, mechanical loading, or large-scale fabrication challenges, which should be addressed in subsequent research.

Acknowledgment

This study was supported by the DIPA Faculty of Engineering at Tadulako University in 2024 with the contract number SP 2653/UN28/KU/2024.

References

[1] C.A. Schoeneberger, C.A. McMillan, P. Kurup, S. Akar, R. Margolis, and E. Masanet, "Solar for industrial process heat: A review of technologies, analysis approaches, and potential applications in the United States," *Energy*, vol. 206, pp. 118083, 2020, doi: 10.1016/J.Energy.2020.118083.

[2] M. A. Rosen and R. Kumar, *Thermal energy storage*, Canada: Nova Science Publishers, 2011, pp. 337–354, doi: 10.37868/sei.v2i2.115.

[3] I. Ait Laasri, Z. Elmaazouzi, A. Outzourhit, and M.O. Mghazli, "Investigation of different topology-optimized fin structures in a cylindrical latent heat thermal energy storage unit," *Thermal Science and Engineering Progress*, vol. 33, pp. 101372, 2022, doi: 10.1016/j.tsep.2022.101372.

[4] L.F. Cabeza, A. de Gracia, G. Zsembinszki, and E. Borri, "Perspectives on thermal energy storage research," *Energy*, vol. 231, pp. 120943, 2021, doi: 10.1016/j.energy.2021.120943.

[5] I. Sarbu and I. Sarbu, "Thermal energy storage," *Advances in Building Services Engineering*, pp. 559–627, 2021, doi: 10.1007/978-3-030-64781-0_7.

[6] R. Mabrouk, H. Naji, A.C. Benim, and H. Dhahri, "A state of the art review on sensible and latent heat thermal energy storage processes in porous media: Mesoscopic Simulation," *Applied Sciences*, vol. 12, no. 14, pp. 6995, 2022. doi: 10.3390/app12146995.

[7] L. Seyitini, B. Belgasim, and C.C. Enweremadu, "Solid state sensible heat storage technology for industrial applications–a review," *Journal of Energy Storage*, vol. 62, pp. 106919, 2023, doi: 10.1016/j.est.2023.106919.

[8] V. Kavimani, P.M. Gopal, T. Thankachan, and V. Sivamaran, "Evolution and recent advancements of composite materials in thermal applications," in *Applications of Composite Materials in Engineering*, Elsevier, 2025, pp. 119–138, doi: 10.1016/B978-0-443-13989-5.00005-X.

[9] A. Kar, A. Sharma, and S. Kumar, "A critical review on recent advancements in aluminium-based metal matrix composites," *Crystals*, vol. 14, no. 5, pp. 412, 2024, doi: 10.3390/cryst14050412.

[10] D.M.R. Prasad, R. Senthilkumar, G. Lakshmanarao, S. Krishnan, and B.S. Naveen Prasad, "A critical review on thermal energy storage materials and systems for solar applications." *AIMS Energy*, vol. 7, no. 4, 2019, doi: 10.3934/energy.2019.4.507.

[11] L.F. Cabeza, I. Martorell, L. Miró, A.I. Fernández, and C. Barreneche, "Introduction to thermal energy storage (TES) systems." *in Advances in Thermal Energy Storage*

Systems: Methods and Applications, Woodhead Publishing Series in Energy, 2015, doi: 10.1533/9781782420965.1.

[12] F. Desai, J.S. Prasad, P. Muthukumar, and M. Rahman, "Thermochemical energy storage system for cooling and process heating applications: A review," *Energy Conversion and Management*, vol. 229, pp. 113617, 2021, doi: 10.1016/j.enconman.2020.113617.

[13] S. Al-Hashmi, M. Chen, and S. Al-Saidi, "Advancing sustainable energy solutions for hot regions: an in-depth exploration of solar thermal energy storage (STES) technologies and applications," *Engineering Research Express*, vol. 7, no. 1, pp. 12101, 2025, doi: 10.1088/2631-8695/adb8a0.

[14] L. Tyagi, R. Butola, and A.K. Jha, "Mechanical and tribological properties of AA7075-T6 metal matrix composite reinforced with ceramic particles and aloevera ash via Friction stir processing," *Materials Research Express*, vol. 7, no. 6, pp. 66526, 2020, doi: 10.1088/2053-1591/ab9c5e.

[15] C.O. Ujah and D.V. Von Kallon, "Trends in aluminium matrix composite development," *Crystals*, vol. 12, no. 10, pp. 1357, 2022, doi: 10.3390/cryst12101357.

[16] P. Gudlur. A. Forness. J. Lentz. M. Radovic. and A. Muliana, "Thermal and mechanical properties of Al/Al_2O_3 composites at elevated temperatures," *Materials Science and Engineering: A*, vol. 531. pp. 18–27, 2012, doi: 10.1016/j.msea.2011.10.001.

[17] E.S.Y. El-Kady, T.S. Mahmoud, and A.A.-A. Ali, "On the electrical and thermal conductivities of cast $A356/Al_2O_3$; Metal matrix nanocomposites," *Materials Sciences and Applications*, vol. 02, no. 09, pp. 1180–1187, 2011, doi: 10.4236/msa.2011.29159.

[18] K. Almadhoni and S. Khan, "Evaluation of the effective thermal properties of aluminum metal matrix composites reinforced by ceramic particles," *International Journal of Current Engineering and Technology*, vol. 5, no. 4, pp. 2884-2897, 2015. Available: http://inpressco.com/category/ijcet.

[19] M.H. Basri, Jalaluddin, R. Tarakka, M. Syahid, A.A. Mochtar, and M.A.I. Ramadhani, "Thermal properties characteristic of aluminium-alumina composite for solar water heating system application," *in Journal of Physics: Conference Series. Institute of Physics*, 2024, doi: 10.1088/1742-6596/2739/1/012018.

[20] S.J. Raab, R. Guschlbauer, M.A. Lodes, and C. Körner, "Thermal and electrical conductivity of 99.9% pure copper processed via selective electron beam melting," *Advanced Engineering Materials*, vol. 18, no. 9, pp. 1661–1666, 2016, doi: 10.1002/adem.201600078.

[21] J. Gayathri and R. Elansezhian, "Influence of dual reinforcement (nano CuO + reused spent alumina catalyst) on microstructure and mechanical properties of aluminium metal matrix composite," *Journal of Alloys and Compounds*, vol. 829, 2020, doi: 10.1016/j.jallcom.2020.154538.

[22] A. Strojny-Nędza, K. Pietrzak, F. Gili, and M. Chmielewski, "FGM based on copper–alumina composites for brake disc applications," *Archives of Civil and Mechanical Engineering*, vol. 2, no. 3, 2020, doi: 10.1007/s43452-020-00079-1.

[23] M. Tayyebi and M. Alizadeh, "Thermal and wear properties of Al/Cu functionally graded metal matrix composite produced by severe plastic deformation method," *Journal of Manufacturing Processes*, vol. 85, pp. 515–526, 2023, doi: 10.1016/j.jmapro.2022.11.059.

[24] G.R. Xu, J.L. Zou, and G.B. Li, "Effect of sintering temperature on the characteristics of sludge ceramsite," *Journal of Hazardous Materials*, vol. 150, no. 2, pp. 394–400, 2008, doi: 10.1016/j.jhazmat.2007.04.121.

[25] D.E. Aldrich and M.J. Edirisinghe, "Addition of copper particles to an alumina matrix," *Journal of Materials Science Letters*, vol. 17, no. 12, pp. 965–967, 1998, doi: 10.1023/A:1006623528590.

[26] E. Villanueva, I. Vicario, I. Crespo, T. Guraya, I. Hurtado, and J. Albizuri, "Development of a new ductile heat-treated multi-component aluminium by HPDC with high-performance properties for temperature applications," *Journal of Alloys and Compounds*, pp. 179146, 2025, doi: 10.1016/j.jallcom.2025.179146.

[27] J. Hu, T. Gao, G. Liu, J. Liu, W. Xu, and X. Liu, "An Al matrix composite reinforced with carbon nanotubes, Al3BC, and γ-Al2O3: Investigation of mechanical, thermal, and wear resistance properties," *Materials Characterization*, pp. 114854, 2025, doi: 10.1016/j.matchar.2025.114854.

[28] S. Madhusudan, M.M.M. Sarcar, and N.B.R.M. Rao, "Mechanical properties of Aluminum-Copper(p) composite metallic materials." *Journal of Applied Research and Technology*, vol. 14, no. 5, pp. 293–299, 2016, doi: 10.1016/j.jart.2016.05.009.

[29] L. Ren, "Molecular dynamics simulation study on thermal conduction of CNT-Cu/Al composites with new MEAM potentials between C and Cu/Al," *Doctoral Dissertation*, 2020. Available: https://purls.library.ucf.edu/go/DP0023577.

[30] K. Ahmad, Z. Almutairi, R. Almuzaiqer, A. AlHazaa, and C. Wan, "Processing and thermal properties of $SrTiO_3/Ti_3AlC_2$ ceramic nanocomposites," Ceramics International, vol. 48, no. 13, pp. 18739–18744, 2022, doi: 10.1016/j.ceramint.2022.03.148

[31] W.A. Shah, X. Luo, and Y.Q. Yang, "Mechanical and thermal properties of spark plasma sintered Al_2O_3-graphene-SiC hybrid composites," *Ceramics International*, vol. 49, no. 5, pp. 7987–7995, 2023, doi: 10.1016/j.ceramint.2022.10.312.